Article

Water Budget of Urban Turf Field and Optimal Irrigation Schedule Simulation in an Ecotone between Semi-Humid and Semi-Arid Regions, Northern China

Hongjuan Zhang [1,2], Jianjun Wang [1,2], Mengzhu Liu [3], Yanjun Shen [3] and Hongwei Pei [1,2,*]

1   Department of Municipal and Environmental Engineering, Hebei University of Architecture, Zhangjiakou 075000, China
2   Hebei Key Laboratory of Water Quality Engineering and Comprehensive Utilization of Water Resources, Zhangjiakou 075000, China
3   Key Laboratory of Agricultural Water Resources, Center for Agricultural Resources Research, Institute of Genetics and Developmental Biology, Chinese Academy of Sciences, Shijiazhuang 050022, China
*   Correspondence: phw1987@126.com; Tel.: +86-185-3312-7087

Abstract: Water security in the ecotone between semi-humid and semi-arid regions (EHA) is very vulnerable and sensitive to climate change and human interferences. Urban turf irrigation is a primary consumer of urban water resources in the EHA, which places huge pressures on water security by substantial irrigated water use due to the expansion of urban turf planting. Based on a 2-year (2020–2021) turf experiment in Zhangjiakou City, a typical water-deficit city in the EHA of northern China, the water budget for turf was measured and analyzed. Furthermore, the Root Zone Water Quality Model (RZWQM2) was employed to evaluate the optimal irrigation scheme for turf. The results showed that the average volumetric water content in the 0–40 cm soil layer was maintained above 23% in 2020–2021. The evapotranspiration in growth period of turf accounted for more than 70% of the annual evapotranspiration, and the deep seepage in turf soil accounted for 49.67% and 60.28% of the total precipitation and irrigation in 2020 and 2021, respectively, during the vigorous growth period of the turf from May to September. The calibrated RZWQM2 showed a robust ability to simulate the water changes in turf. The d-values (consistency index) between the simulated and observed volumetric water contents and evapotranspiration were both greater than 0.90. In the aspects of irrigation scenarios, the $T_{60\%-12}$ scenario (T_{A-B}, where A is 100%, 80%, 60% or 40% of the total irrigation amount and B is the number of irrigation events corresponding to A) was determined as the best irrigation schedule in our study area because of lower evapotranspiration, seepage and higher turf soil water storage under this irrigation scenario, also resulting from the comparison of different irrigation scenarios using the entropy-weight-TOPSIS method. In such an optimal scenario, $T_{60\%-12}$ irrigation treatment reduced the irrigated water requirement of turf by 40% (142.06 mm) and the seepage amount by 28.07% (39.05 mm), and had the lowest negative impacts on the turf growth.

Keywords: RZWQM2; urban turf; applicability; irrigation schedule

1. Introduction

Water shortage is a main factor restricting China's economic and social development and ecological conservation. China's water resources are only 2876.12 billion m³, accounting for 5.1% of the world's water resources; additionally, China's per capita available water resource is only 1/4 of the world's total [1]. Furthermore, China's urbanization rate increased from 17.9% to 58.5% from 1978 to 2017, resulting in a sharp increase in per capita daily water consumption with a significant increase from 117 L/day to 221 L/day that period [2].

The area of China's urban turf planting increased from 1.3 million ha in 2006 to 3.2 million ha in 2019, an increase of 141.67%. Taking Zhangjiakou City of northern China as a case, the urbanization development has unprecedentedly accelerated in the past two decade, and the rate of urban greening increased from 25% in 1996 to 38% in 2017. The turf planting region in some cities and counties of northern China increased by at most 1.76 million m^2 annually [3]. With the rapid expansion of urban turf planting, water resources are severely overused due to the excessive turf irrigation and unreasonable turf management systems, especially in water-deficit cities in northern China. As a result, the storage of water resources has been neglected, which severely threatens urban water security [4]. Zhangjiakou City is located in the semi-humid and semiarid region in northern China, with a multi-year average water resource of 1.54 billion m^3 and a per capita rate of only 347 m^3 available water, far less than 1/5 of the national level. Hence, for such a typical water-deficit region in northern China [5], it is critical to examine turf water-saving irrigation to improve the utilization of urban water resources in response to the growing pressures on urban water shortages.

An optimal turf irrigation schedule can achieve efficient irrigation water use by adjusting irrigated water to reduce evapotranspiration and seepage [6,7]. The key to an optimal turf irrigation schedule is appropriately allocating the amount of irrigation, irrigation quotas and the number of irrigation cycles over the turf growing period [8]. Therefore, a reasonable turf irrigation schedule not only improves the efficiency of urban water-saving, but also maximizes economic benefits. In the traditional irrigation system, field experiments are widely used to assess the changes of water consumption and volumetric water content to determine the optimal irrigation quota and amount, which requires a long experimental period and faces many unpredictable experimental impacts. Specific model-based methods can overcome these drawbacks and effectively simulate water dynamics.

The root zone water quality model (RZWQM2) has become a promising tool for agricultural water management since its inception in 1992 [9] and has been applied to optimize field management practices for crop growth under different irrigation conditions [10]. RZWQM2 has performed well in simulating crop growth and volumetric water content (VWC) under different irrigation conditions [11]. RZWQM2 has been widely adopted in many studies on crop growth [12–14], and it can simulate pesticide residues [15], nitrogen fertilizer uptake [16], crop growth processes [17], crop transpiration processes [18] and crop water use efficiency [19]. RZWQM2 was calibrated and validated using winter wheat growth data from 2015 to 2019 [20]. Field trials have disadvantages such as long lead times and complicated repeatability [21], but RZWQM2 can address these disadvantages [22], and hence the model has become a powerful tool for agricultural research; in addition, it has been widely used in different fields, such as irrigation management optimization, crop growth simulation, crop yield prediction and environmental evaluation [10].

In this study, 16 turf irrigation scenarios were designed and applied in RZWQM2 to explore optimal irrigation water amount and frequency. Meteorological data from 2000–2021 were used to drive RZWQM2. The main objectives of this study are to (1) analyze the applicability of RZWQM2 in simulating turf water consumption, (2) investigate the response of soil water storage, evapotranspiration variations and water seepage change under different irrigation schedules, and (3) explore the optimal irrigation schedule for urban turf in arid areas.

2. Materials and Methods

2.1. Experimental Site

This experiment site is at the Hebei University of Architecture, Zhangjiakou City (40°45' N, 114°54' E), and the study periods cover the turf growing season in 2020 and 2021. The experiment site is located in the arid and semiarid regions of northern China, with an annual average precipitation of 401.3 mm (1960 to 2016). In the turf growing season in 2020 and 2021, the total precipitation was 444.09 mm and 342.72 mm (Figure 1), respectively. The experiment plot utilized the *Poa pratensis* turf species, which is commonly used in the

northern region. The soil texture of this experiment region was homogeneous sandy loam with a soil pH value of 8.51, fast-acting potassium of 74 mg/kg, fast-acting phosphorus of 5 mg/kg, and organic matter of 7.8 g/kg, while the contents of cations (including Na^+, K^+, Mg^{2+}, and Ca^{2+}) in the soil were 46, 8, 10, and 98 mg/kg, respectively, and the contents of anions (including F^-, Cl^-, and NO^{3-}) were 8, 22, and 19 mg/kg, respectively. The soil conductivity was 131 μs/cm.
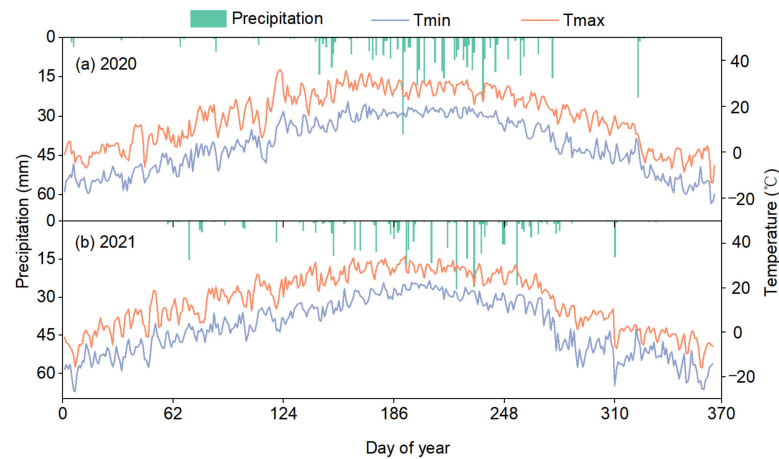

Figure 1. Precipitation, maximum (Tmax) and minimum (Tmin) air temperature in the experimental field (2020 and 2021, the datasets were from the HOBOU-30 meteorological station).

2.2. Information on Turf Management

The turf species *Poa pratensis* was planted in June 2019. It is commonly planted in northern regions. The plot size was 0.8 m × 0.8 m, and a large weighing lysimeter was installed at the bottom of the plot, which consists of a 0.8 m × 0.8 m × 1.2 m iron box (Figure 2). Total irrigation volume was 23.4 mm and 203.7 mm in 2020 and 2021, respectively. The low amount of irrigation in 2020 was mainly due to high rainfall and frequent precipitation during the turf growing season in 2020, and hence only two irrigation events were used. Fertilizers were applied twice in 2020–2021, both with "compound fertilizers". At the same time, turf management such as mowing, weed removal and fertilization were regularly carried out on the turf in the test plot.
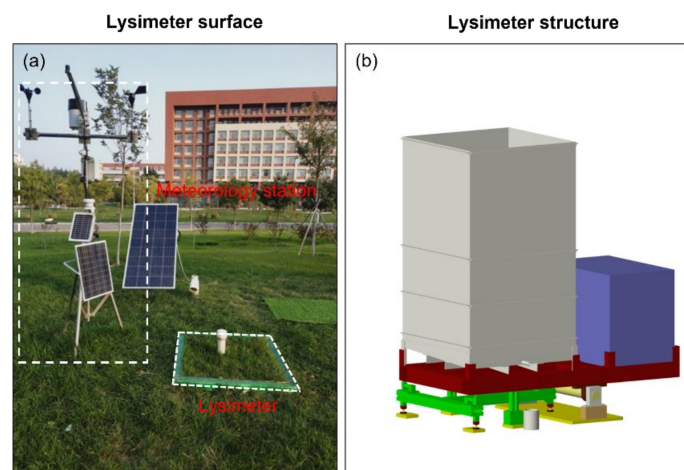

Figure 2. Above-ground part and underground part of turf field experiment. ((**a**) represents the above-ground part of the lysimeter; (**b**) represents the structure diagram of the lysimeter).

2.3. Data Collection

2.3.1. Meteorological Data

The meteorological data during the turf growth period were measured by a Hobo mini-weather station installed in this experiment site and included daily maximum and minimum temperature (°C), daily average temperature (°C), precipitation (mm), relative humidity (%), wind speed (m/s) and sunshine hours (h). The daily radiation was determined by an integrated module based on the Penman-Monteith method [23]. A long-term historical meteorological data (2000–2021) covering the study region was gained from the China Meteorological Data Service Center (http://data.cma.cn, accessed on 10 September 2022).

2.3.2. Soil Data

The soil data included soil texture parameters, soil bulk density, field capacity water content, saturated hydraulic conductivity and volumetric water content for each soil layer. The initial soil data included the initial soil temperature and volumetric water content for each soil layer. The volumetric water content of each soil layer was measured by Insentek-sensors [24], which record the data every 1 h. The soil water content monitoring in this study was performed using Insentek-sensors, which can monitor the change of soil at depths of 0–120 cm at 10-cm intervals. At the same time, the sensor was calibrated and tested for stability when the test equipment was installed, and the collected daily scale data was processed with hourly average data to eliminate the error in the data. In this study, the data in the 20 cm, 40 cm, 60 cm and 80 cm soil layers were selected for analyses.

2.3.3. Experimental Management

The turf data include turf species, planting date, planting density, tillage method, fertilizer application date, irrigation amount and irrigation date, mowing date, mowing height and stubble height, all relevant turf measurement parameters.

2.4. RZWQM2 Description

Developed by the USDA Agricultural Research Service, RZWQM2 is an agricultural system model that integrates biological, physical and chemical processes as a whole [25,26], including the physical, chemical, pesticide, nutrient, crop growth and crop management modules, which interact and influence each other [10,27]. RZWQM2 can provide accurate simulations of water and fertilizer transport during agricultural production, crop responses to changes of soil moisture, and pesticide transport processes in the process of crop growth [28–30]. After calibration, the model can accurately simulate crop growth and development, volumetric water content, and crop evapotranspiration at a daily scale [31]. Therefore, the model can also provide more accurate irrigation decisions for different irrigation measures [32].

Based on the requirements of RZWQM2, databases of local meteorological data, turf data, soil data, turf management data and other turf parameters were established. This study was based on field observations and model simulation using default parameters in 2020 and 2021, and the model parameters were calibrated using a "trial and error" approach due to the small number of calibration parameters required for this study. Only soil physical parameters and volumetric water content were calibrated in this model, and the calibration results are shown in Table 1. In this experimental study, the main physical parameters of the model (Table 1) were calibrated based on the actual soil type and validated by the monitored soil water content. Therefore, the soil physical parameters were chosen to calibrate the model default parameters.

Table 1. Main physical parameters of different soil depth in the experimental site.

Soil Depth (cm)	Soil Texture (%)			Bulk Density (g·cm^{-3})	Saturated Hydraulic Conductivity (cm·h^{-1})	Field Capacity Water Content (cm^3·cm^{-3})
	Sand	Silt	Clay			
20	31.5	48.7	19.8	1.457	3.32	0.3435
40	31.2	47.5	21.3	1.414	2.16	0.3506
60	29.0	52.5	18.5	1.409	1.35	0.3534
80	20.0	65.0	15.0	1.322	0.68	0.3555

2.5. Model Performance Criteria and Calculations

The evaluation indicators of model simulation were utilized in the study region [33,34], including Root Mean Relative Error (*RMSE*), Mean Relative Error (*MRE*) and consistency index (*d*). These statistical criteria are defined as follows:

$$RMSE = \sqrt{\frac{1}{n} \sum_{i=1}^{n} (P_i - Q_i)^2} \tag{1}$$

$$MRE = \frac{1}{N} \sum_{i=1}^{N} \left| \frac{P_i - Q_i}{Q_i} \right| \times 100\% \tag{2}$$

$$d = 1 - \left[\frac{\sum_{i=1}^{n} (P_i - Q_i)^2}{\sum_{i=1}^{n} (|P_i - Q_{avg}| + |Q_i - Q_{avg}|)^2} \right] \tag{3}$$

where P_i is the ith simulated value; Q_i is the ith measured value, Q_{avg} is the average measured value; and *n* is the number of data.

The smaller the *RMSE* value, the better the simulated value fits the measured value and the better the simulation result [35]. The smaller the value of *MRE*, the more standard the simulation results are [36]. The consistency index d value lies between 0 and 1. The closer the d value is to 1, the better the consistency between the measured and simulated values [37].

2.6. Simulation Schedule Design

This study is based on the principles of water balance, the difference between water income and expenditure at a given moment and in a given soil layer, which is a calculation of farm water income, expenditure and storage [38,39]. As the main basis for determining irrigation time and volume, it can respond to soil moisture changes [40], which is defined by the following equation.

$$\Delta W = (P + I + M) - (E + T + R + D) \tag{4}$$

where ΔW is the amount of volumetric water content change (mm); *P* is the amount of precipitation (mm); *I* is the amount of irrigation (mm); *M* is the amount of groundwater recharge (mm); *E* is the amount of soil evaporation (mm); *T* is plant transpiration (mm); *R* is surface runoff; *D* is soil water seepage (the depth of the lysimeter box was 1.2 m).

The sum of soil evaporation and plant transpiration is *E + T = ET*, which is the total evapotranspiration. Since the terrain in this study region is flat and the surface runoff is not considered, while the water table is deep. Therefore, groundwater recharge is also not considered, so the equation can be simplified as:

$$\Delta W = (P + I) - (ET + D) \tag{5}$$

The design of the irrigation regime in this study RZWQM2 is based on the potential evapotranspiration (ET_0), which is calculated by the following equation:

$$I = ET_0 - P \tag{6}$$

where ET_0 is then calculated from the FAO Penman–Monteith method.

A total of 16 different irrigation scenarios ($T_{100\%-12}$ to $T_{40\%-21}$) were set, and four irrigation frequencies (12, 15, 18, 21) were identified based on four irrigation ceilings (100%, 80%, 60%, 40%) and four calculated irrigation quotas (355.14 mm, 284.11 mm, 213.08 mm, 142.07 mm), setting irrigation dates based on the precipitation variation in the region (Table 2). For example, the $T_{100\%-12}$ means the upper limit of irrigation is 100% and the number of irrigation events is 12.

Table 2. Schedules of different irrigation systems for turf.

Irrigation Scenarios	Irrigation Cap/%	Irrigation Quotas/mm	Number of Irrigations	Sub-Irrigation Volume/mm
$T_{100\%-12}$		355.14	12	29.60
$T_{100\%-15}$		355.14	15	23.68
$T_{100\%-18}$	100%	355.14	18	19.73
$T_{100\%-21}$		355.14	21	16.91
$T_{80\%-12}$		284.11	12	23.68
$T_{80\%-15}$		284.11	15	18.94
$T_{80\%-18}$	80%	284.11	18	15.78
$T_{80\%-21}$		284.11	21	13.53
$T_{60\%-12}$		213.08	12	17.76
$T_{60\%-15}$		213.08	15	14.21
$T_{60\%-18}$	60%	213.08	18	11.84
$T_{60\%-21}$		213.08	21	10.15
$T_{40\%-12}$		142.07	12	9.47
$T_{40\%-15}$		142.07	15	7.58
$T_{40\%-18}$	40%	142.07	18	6.31
$T_{40\%-21}$		142.07	21	5.41

2.7. Construction of Irrigation Evaluation Index System

2.7.1. Evaluation Indicators and Methods

The entropy method compares the same indicators of different objects, and to understand the amount of information contained in them by weighting, which may also have a more complex situation, with enhanced objectivity [41]. The TOPSIS method is a system analysis method, which is widely cited in solving multi-target decision-making analysis by judging the approach of research goals and the approach of "positive ideals" and "negative ideals". If the research object is close to the ideal solution, the plan is a better solution in the alternative scheme [42].

In this study, there are four evaluation indicators: irrigation, soil water storage, evapotranspiration and seepage volume. Different indicators were analyzed and optimization solutions were obtained by SPSSAU online.

2.7.2. Determining the Weights of Evaluation Indicators

The weight of the evaluation index is determined by the entropy weight method, and its calculation steps are as follows:

$$X = \begin{bmatrix} x_{11} & \cdots & x_{1n} \\ \vdots & \ddots & \vdots \\ x_{m1} & \cdots & x_{mn} \end{bmatrix} \tag{7}$$

$$r_{ij} = \frac{[X_{ij} - min(X_{ij})]}{[max(X_{ij}) - min(X_{ij})]} \tag{8}$$

$$r_{ij} = \frac{[max(X_{ij}) - X_{ij}]}{[max(X_{ij}) - min(X_{ij})]} \tag{9}$$

where i is the evaluation scheme, j is the evaluation index; *Xmax* and *Xmin* are the maximum and minimum values, respectively, of the jth index in each scheme.

Through the above transformation, the standardized eigenmatrix is obtained as follows:

$$R = \begin{bmatrix} r_{11} & \cdots & r_{1n} \\ \vdots & \ddots & \vdots \\ r_{m1} & \cdots & r_{mn} \end{bmatrix} \tag{10}$$

2.7.3. Evaluation of Entropy Weight-TOPSIS Model

(1) Entropy method to determine the weight

Defining entropy: In a scheme with m indicators and n evaluations, the entropy of the ith indicator is:

$$h_i = -k \sum_{j=1}^{n} f_{ij} \ln f_{ij} \tag{11}$$

where is $f_{ij} = \frac{r_{ij}}{\sum_{j=1}^{n} r_{ij}}$, $k = \frac{1}{\ln n}$, n represents the number of possible states of the system, f_{ij} represents the probability of a certain state of the system.

Defining entropy weight: After defining the entropy of the i-th index, the entropy weight of the i-th index can be obtained as follows:

$$w_i = \frac{1 - h_i}{m - \sum_{i=1}^{m} h_i} \left(0 \leq w_i \leq 1, \sum_{i=1}^{m} w_i = 1 \right) \tag{12}$$

where h_i is the entropy of the i-th index, w_i is the entropy weight of the ith index.

(2) Construction of evaluation matrix

$$Z = \begin{bmatrix} z_{11} & \cdots & z_{1n} \\ \vdots & \ddots & \vdots \\ z_{m1} & \cdots & z_{mn} \end{bmatrix} = \begin{bmatrix} r_{11}w_1 & \cdots & r_{1n}w_n \\ \vdots & \ddots & \vdots \\ r_{m1}w_1 & \cdots & r_{mn}w_n \end{bmatrix} \tag{13}$$

(3) TOPSIS determines the distance of the index to the positive and negative ideals

$$D_j^+ = \sqrt{\sum_{i=1}^{m} \left(z_i^+ - z_{ij} \right)^2} \tag{14}$$

$$D_j^- = \sqrt{\sum_{i=1}^{m} \left(z_i^- - z_{ij} \right)^2} \tag{15}$$

where z_i^+ and z_i^- are the maximum and minimum values of the nth column of the normalized weighting matrix.

(4) Calculation of the comprehensive evaluation index

$$C_j = \frac{D_j^-}{D_j^+ + D_j^-} \tag{16}$$

The closer C is to 1, the better the evaluation object.

3. Results and Discussion

3.1. Water Balance Analysis

3.1.1. Volumetric Water Content Variation in Different Soil Profiles

Figure 3 shows the variation in VWC in the 0–100 cm soil layer in the turf growth season from 2020 to 2021. The VWC exhibited an increasing trend in the observed period, and the average VWC values at the depth of 0–40 cm soil layer were 23.24% and 23.27% during the precipitation and irrigation periods in 2020 and 2021, respectively. At the same time, the VWC value was lower in the 40–60 cm soil layer than in the 0–40 cm soil layer, reaching 19.70% and 20.39%, respectively. The annual precipitation was concentrated from April to October annually in the study region, during which the amount of annual

precipitation was 394.64 mm and 310.20 mm in 2020 and 2021, respectively, accounting for 88.87% and 91.58% of the total annual precipitation (444.09 mm and 342.72 mm), respectively. The main irrigation was carried out during this period, thus making the volumetric water content in the 0–40 cm soil layer greater than that in the 40–60 cm soil layer. In contrast, the average volumetric water content in the 70–100 cm soil layer in 2021 (mean value 26.54%) was significantly lower than that in 2020 (32.63%), mainly because the precipitation during the turf growing period in 2021 was significantly lower than that in 2020. The precipitation in 2021 was 310.20 mm, which was 84.44 mm less than that in 2020. The VWC below the 80 cm soil layer was thought to have reached a saturated state. Overall, the average VWC in the 0–40 cm soil layer from 2020 to 2021 was higher in the rainy season than in the other seasons, while the average VWC in each soil layer was lower when soil freezing and thawing occurred in winter.
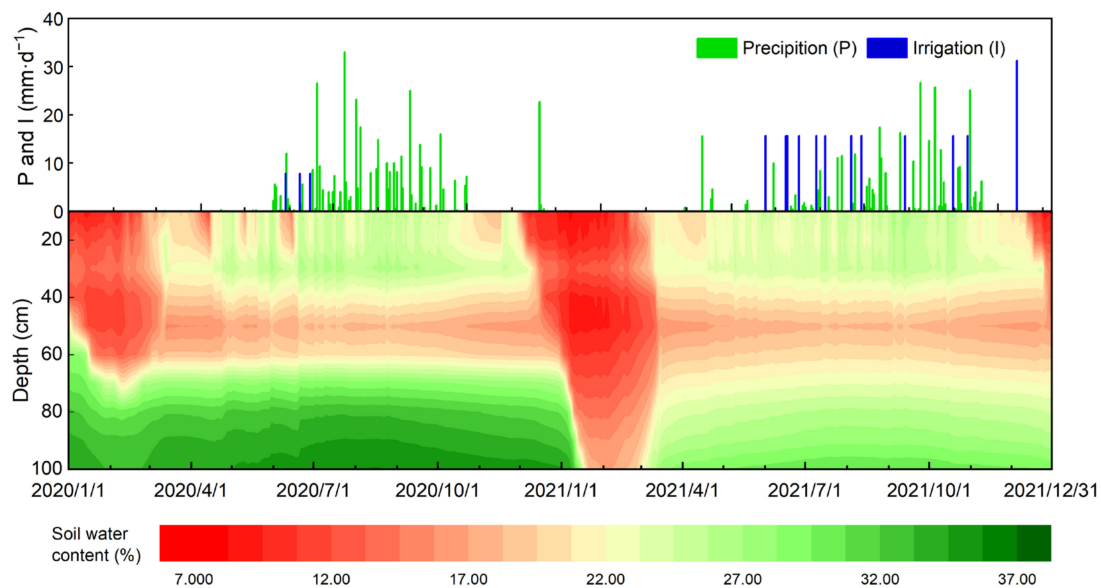

Figure 3. Variation of volumetric water content (VWC) in the 0–100 cm soil layer.

The main reason for the low water content in winter is that the soil water content appeared to be frozen by shrinkage due to very low winter temperatures at the experiment site. From the perspective of results, water content consumption by turf in the 0–40 cm soil layer was dominant, and soil water content under the 60–100 cm soil layer was basically not used by turf. The results of this study were similar to the results of soil water content changes of turf in the Beijing area [43].

3.1.2. Variation in Evapotranspiration under at Varying Time Scales

Figures 4 and 5 show the variations in the daily evapotranspiration, cumulative evapotranspiration and monthly evapotranspiration in the study period. The annual evapotranspiration of the turf first increased and then decreased. The evapotranspiration maximum of the turf occurred in June, and the maximum values were 9.15 mm in 2020 and 7.01 mm in 2021. These values were observed mainly because of the more frequent irrigation events and a greater irrigation water volume in June 2021 than in 2020; in addition, higher temperatures and turf water consumption occurred in the peak growth period. The total evapotranspiration of turf was 634.92 mm and 496.80 mm from May to September in 2020 and 2021, respectively, accounting for 75.34% and 72.80% of the total evapotranspiration, respectively. At the same time, the total evapotranspiration was 842.74 mm in 2020 and 682.40 mm in 2021. The average rates of turf evapotranspiration in June were 5.86 mm/d in 2020 and 4.57 mm/d in 2021. However, the evapotranspiration was low in winter (November–March) at less than 10% of the total evapotranspiration. In addition, the total evapotranspiration in winter was 40.08 mm and 50.47 mm in 2020 and 2021, respectively,

accounting for 4.76% and 7.40% of the annual evapotranspiration, respectively, mainly due to the soil freezing and thawing in winter when the turf leaves wilted and the temperature was low. Therefore, the evapotranspiration in winter is considered to result from soil evaporation. The results of turf evapotranspiration mainly showed an overall trend of increasing and then decreasing during the peak growth period, similar to Ross's results [44] on evapotranspiration of cool-season lawns in response to water deficit irrigation.
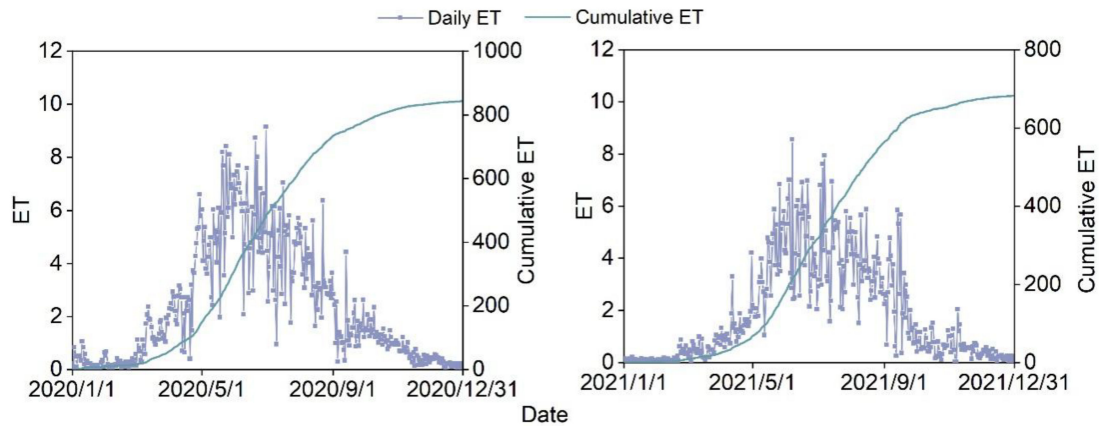

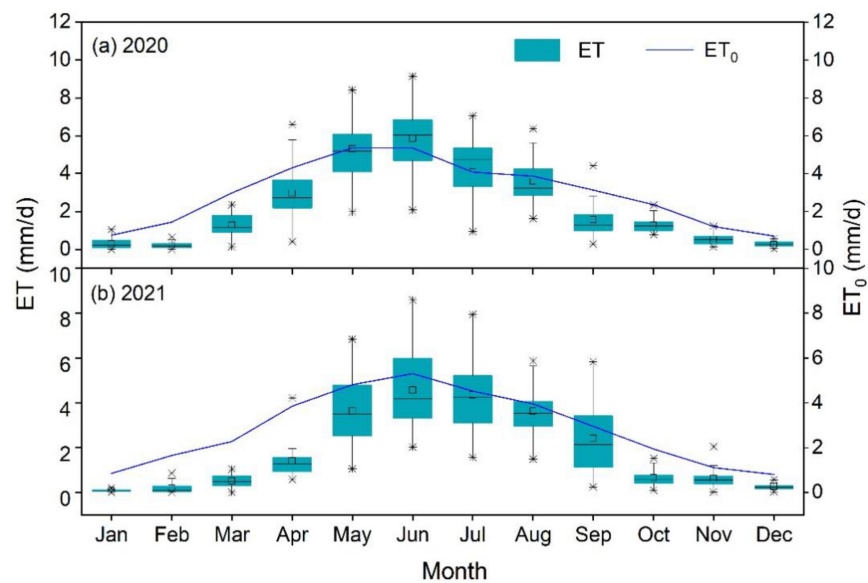**Figure 4.** Variations of evapotranspiration (ET) and cumulative ET in 2020 and 2021.

Figure 5. Evapotranspiration (ET) changes at the turf experiment site during 2020 (**a**) and 2021 (**b**). The top and bottom range of the box represent the 25th and 75th percentiles. The box whisker represents an outlier ranger and stars are extrema. The line and square within the box represent medium and mean values, respectively.

3.1.3. Seepage Variation

Figure 6 shows the variation in seepage and cumulative seepage from 2020–2021. Daily seepage varied with the changes of precipitation and irrigation in the turf growth period when the cumulative seepage amounts reached 232.74 mm in 2020 and 332.64 mm in 2021.
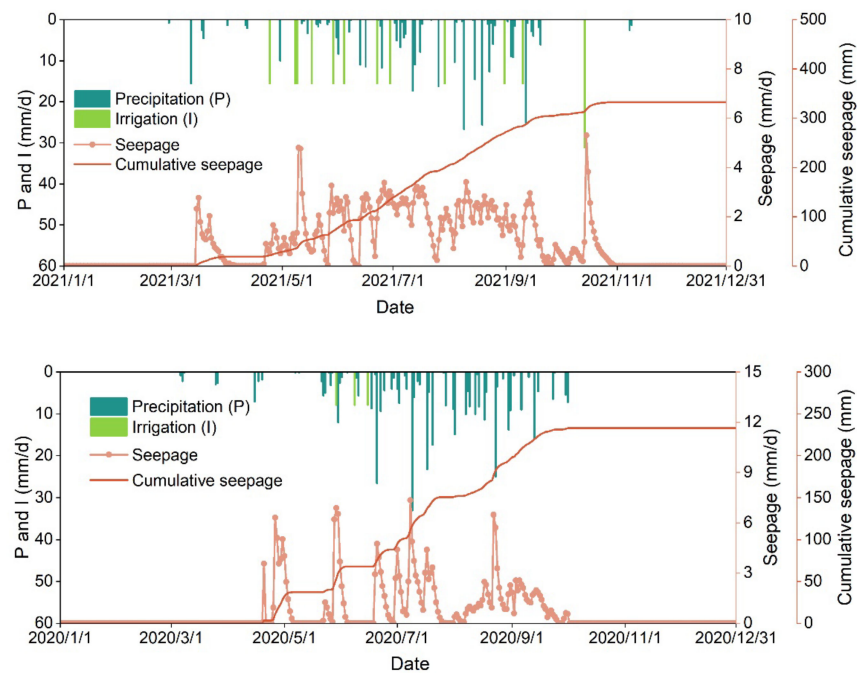
Figure 6. Variations of seepage and cumulative seepage in turf growth period with precipitation and irrigation conditions in 2020 and 2021.

The seepage in the turf field was mainly concentrated from May to October, during which the frequent precipitation and irrigation events occurred. The daily seepage maximum was 7.35 mm in 2020, with the greatest precipitation reaching 33.0 mm. In addition, 45.72 mm of monthly seepage with 125.60 mm of precipitation occurred in August 2020. At the same time, the highest monthly seepage of 59.88 mm was in July 2020, accounting for 25.73% of the total seepage. The cumulative seepage in 2021 was 332.64 mm, an increase of 99.90 mm compared to that in 2020, mainly due to the increase in irrigation in 2021 of 203.19 mm and 12 events. The total seepage amounts in July and August in 2021 were approximately the same at 66.63 mm and 66.75 mm, respectively, and the total precipitation and irrigation in August was 116.53 mm, followed by 60.74 mm in June.

During the mature stage of turf, the daily seepage gradually increased, especially after precipitation and irrigation events, while the daily seepage amount decreased when precipitation was low, so that the higher seepage amount occurred mainly in July and August when precipitation was high; in addition, no seepage occurred during winter and rainless periods.

3.2. Model Calibration and Validation Results

Simulation of Volumetric Water Content

In this study, the volumetric water content in 2021 was selected as the validation period for RZWQM2. The dynamic changes in turf volumetric water content at different soil profile depths (20 cm, 40 cm, 60 cm, and 80 cm) were simulated in the key growing period of turf (May–October) after the soil hydraulic parameters were adjusted periodically. The measured volumetric water content data before and after precipitation and irrigation were selected as the volumetric water content data for the validation period. The volumetric water content at depths of 40 cm, 60 cm and 80 cm soil layers fluctuated at 20–22%, 19–21% and 24–26%, respectively, without significant variability.

Figure 7 shows the comparison between the VWC in the 0–80 cm soil layer and the corresponding value simulated by RZWQM2. In this study, VWC data from 2020 were used for the model calibration, and volumetric water content data for 2021 were used to verify the modeled results. The simulation period covered the 2020–2021 turf growing seasons. To calibrate the modeled VWC in 2020, the simulated value overall corresponded

to the measured value. The d-values were all greater than 0.80, and the mean relative errors (*MRE*s) were 8.33%, 5.19%, 4.04% and 1.48% in the 20 cm, 40 cm, 60 cm and 80 cm soil layers, respectively. The simulated results were consistent with the calibrated results, and the *RMSE* was greater than 1.5%. At the same time, the d-values of VWC simulation at the 20 cm, 40 cm, 60 cm and 80 cm soil layers were all greater than 0.90. As shown in Figure 3, the simulated values better reflected the trend in the measured values and the fluctuation in VWC in the different soil layers.
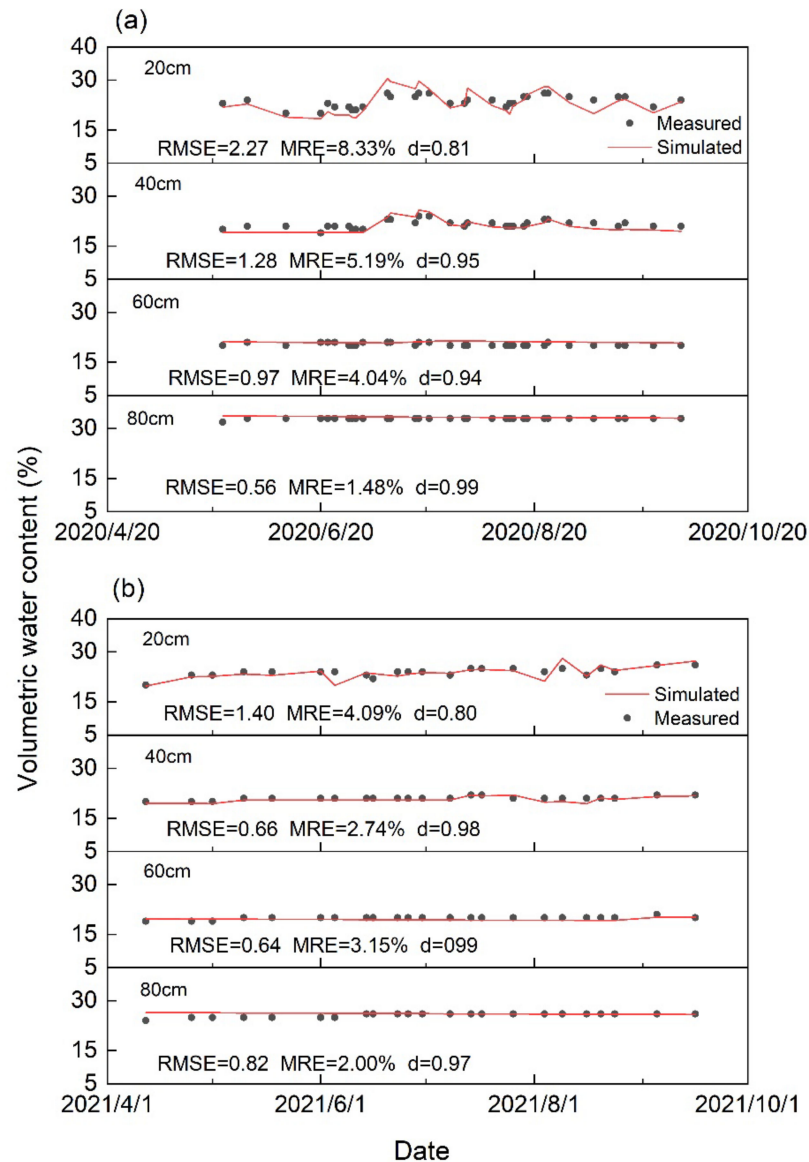

Figure 7. Comparison between measured volumetric water content (VWC) in the 20 cm, 40 cm, 60 cm and 80 cm profile the simulated values by RZWQM2 during the growth period of turf in 2020 (**a**) and 2021 (**b**).

The *RMSE* values of the simulated VWC of each soil layer in 2020 were less than 3.00%, reaching 2.27%, 1.28%, 0.97% and 0.56% at depths of 20 cm, 40 cm, 60 cm and 80 cm soil layers, respectively, and accordingly, the *MRE* values were 8.33%, 5.19%, 4.04% and 1.48%, respectively. The d-values of the simulated VWC were 0.81, 0.95, 0.94 and 0.99 in the four soil layers. In 2021, the simulated VWC values at the 40 cm, 60 cm and 80 cm soil layers were higher than those at the 20 cm soil layer, and the d-values reached 0.98, 0.99 and 0.97, respectively, with the *RMSE* values reaching 0.66%, 0.64% and 0.82% and *MRE* values reaching 2.74%, 3.15% and 2.00%, respectively. Overall, RZWQM2 showed good

applicability in simulating turf water uses in this region. Compared with that of the surface soil, the VWC at the deep soil layer was better simulated by RZWQM2, and the simulated error was relatively low. Similarly, the VWC simulation of the surface layer (20 cm) was relatively poor, as the surface soil layer is affected by the external environment [44,45]. In this study, the simulation of RZWQM2 for the water content of the surface layer may have a large error compared to other soil layers. The possible reason for this is the error due to external factors, such as the idealized turf growth in the model and the actual turf growth in the field, which resulted in the poor simulation of soil water content in the surface layer [46].

Figure 8 shows the simulation of evapotranspiration during the turf growth period from 2020 to 2021. The d-values between the simulated and observed monthly evapotranspiration reached 0.92 and 0.91 (both >0.90) in 2020 and 2021, respectively. The simulated *RMSE* and *MRE* values were low as a result of the *RMSE* values (22.08 mm and 12.60 mm) and the *MRE* values (5.22% and 9.94%) in 2020 and 2021, respectively. Overall, the simulated and measured values of turf evapotranspiration in 2021 and 2021 were highly consistent. In comparison to the measured values, RZWQM2 better simulated turf evapotranspiration, and the results show that RZWQM2 has better applicability in this region.
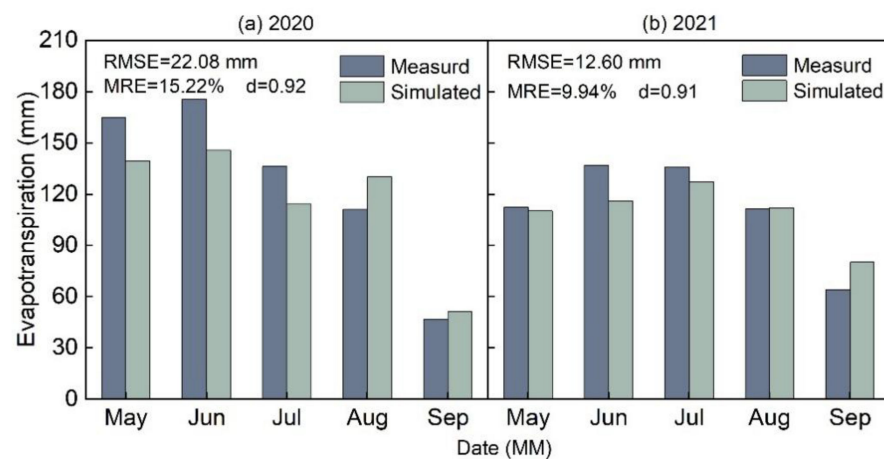

Figure 8. Comparison between measured evapotranspiration (ET) and simulated values by RZWQM2 during the growth period of turf in 2020 and 2021.

3.3. Response Simulation of Different Irrigation Schedules

3.3.1. Soil Water Storage

Figure 9 shows the comparison of soil water storage (SWS) in different irrigation schedules. In 16 different turf irrigation schedules, the overall SWS showed low fluctuations from May to August and a significant increase from August to October.

The SWS for different scenarios were ranked as: $T_{100\%-12} > T_{80\%-12} > T_{60\%-12} > T_{40\%-12}$, $T_{100\%-15} > T_{80\%-15} > T_{60\%-15} > T_{40\%-15}$, $T_{100\%-18} > T_{80\%-18} > T_{60\%-18} > T_{40\%-18}$ and $T_{100\%-21} > T_{80\%-21} > T_{40\%-21}$. Less SWS occurred from May to August, mainly due to the considerable water consumption resulting from high air temperatures and turf evapotranspiration in this period. The average values of SWS were 194.73 mm, 197.46 mm, 199.26 mm and 199.49 mm under $T_{100\%-21}$, $T_{80\%-21}$, $T_{60\%-21}$ and $T_{40\%-21}$ treatments, respectively, and the SWS maximum was observed in the $T_{100\%-21}$ treatment. The maximum average values of SWS were observed in the $T_{80\%-21}$, $T_{60\%-21}$ and $T_{40\%-21}$ schedules under 80%, 60% and 40% irrigation conditions, respectively. Compared with the fully irrigated treatment, the maximum of average SWS decreased by 3.00%, 6.21% and 8.06% under the irrigation treatments of $T_{80\%-21}$, $T_{60\%-21}$ and $T_{40\%-21}$, respectively. The average values of SWS in the $T_{80\%-21}$ and $T_{80\%-18}$ treatments were only 0.70% and 0.63%, respectively, which were lower than those in the $T_{100\%-12}$ treatment under fully irrigated treatment. Therefore, compared with the full irrigation treatment, $T_{80\%-18}$ and $T_{80\%-21}$ irrigation treatments under 80% irrigation conditions were better.
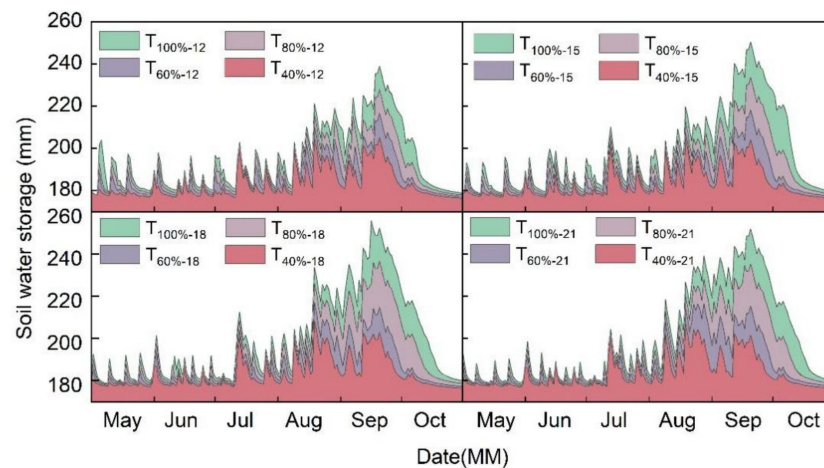
Figure 9. Simulation and comparison of soil water storage (SWS) under different irrigation conditions.

3.3.2. Total Evapotranspiration

Figure 10 shows the comparison of total evapotranspiration in the different irrigation treatments. The trends of the simulated evapotranspiration values were generally similar. The overall trend showed the highest evapotranspiration at the 18 irrigation frequency and the lowest evapotranspiration at the 21 irrigation frequency.
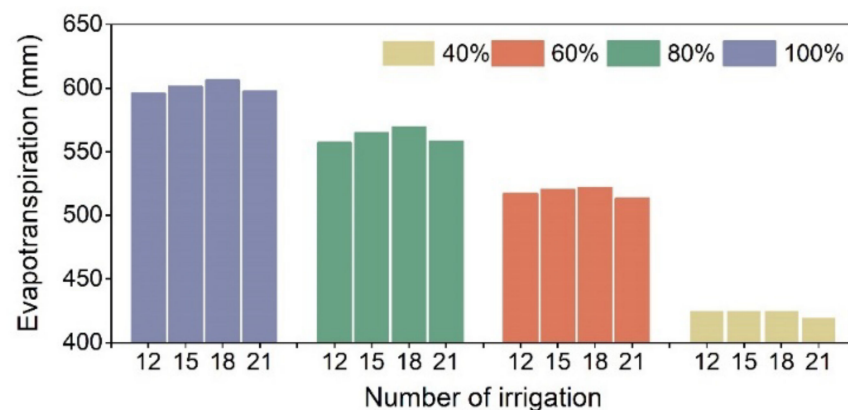

Figure 10. Simulation and comparison of total evapotranspiration under different irrigation conditions.

The total evapotranspiration values under different irrigation treatments were ranked as $T_{100\%-18}$ (595.88 mm) > $T_{100\%-15}$ (601.35 mm) > $T_{100\%-12}$ (606.31 mm) > $T_{100\%-21}$ (597.75 mm), and the maximum of turf evapotranspiration was 606.30 mm under full irrigation treatment. The maximum of total evapotranspiration was 569.55 mm, 521.87 mm and 425.37 mm for the $T_{80\%-18}$, $T_{60\%-18}$ and $T_{40\%-18}$ treatments, respectively, under 80%, 60% and 40% irrigation treatments. Compared with the full irrigation treatment, the irrigation conditions of $T_{80\%-18}$, $T_{60\%-18}$ and $T_{40\%-18}$ resulted in the decrease of total evapotranspiration maxima by 6.06%, 13.93% and 29.84%, respectively. Therefore, the total evapotranspiration was close to the maximum of total evapotranspiration in the $T_{80\%-15}$, $T_{80\%-18}$ and $T_{80\%-21}$ irrigation treatments compared with that in the full irrigation treatment, and the $T_{80\%-18}$ irrigation treatment was better than the $T_{80\%-15}$ and $T_{80\%-21}$ treatments. Therefore, the $T_{80\%-18}$ irrigation treatment was better in terms of the decrease in overall evapotranspiration.

3.3.3. Cumulative Seepage

Figure 11 shows the comparison of cumulative seepage in the different turf irrigation treatments, and the variation trends of the simulated cumulative seepage were entirely consistent. Each trend has increased under the four irrigation treatments of 100%, 80%, 60% and 40%.
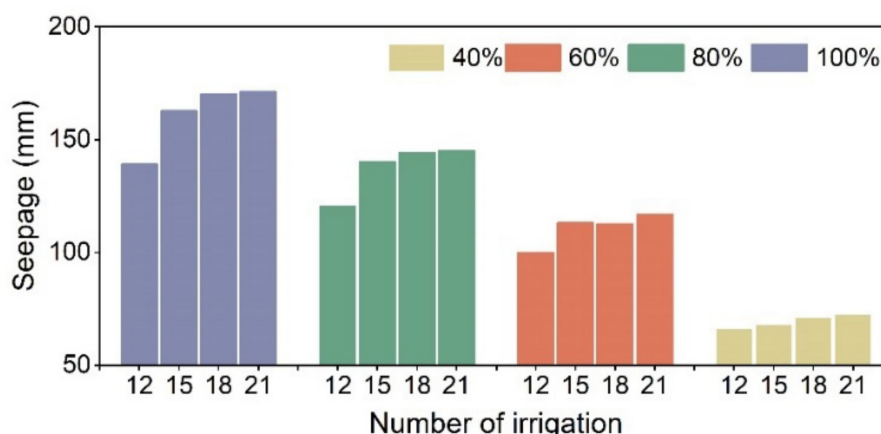
Figure 11. Simulation and comparison of cumulative seepage under different irrigation schedules.

With the increase in irrigation frequency, the cumulative seepage also increased gradually, and it scarcely increased when the irrigation frequencies were 18 and 21. The cumulative seepage values under the $T_{80\%-18}$ and $T_{80\%-21}$ irrigation treatments were 170.30 mm and 171.21 mm, respectively, with an increase of only 0.57%. From the analysis of the changes in SWS and total evapotranspiration, the $T_{80\%-18}$ and $T_{80\%-21}$ irrigation treatments reduced cumulative seepage most significantly, as the simulated cumulative seepage of the $T_{80\%-18}$ and $T_{80\%-21}$ irrigation treatments was 144.31 mm and 144.95 mm, respectively. Therefore, the $T_{80\%-18}$ irrigation treatment was better than the $T_{80\%-21}$ irrigation schedule.

3.4. Entropy Weight-TOPSIS Method to Evaluate Optimal Irrigation Schedule

Table 3 showed the relative proximity of different irrigation schedules. Among them, the relative proximity of the $T_{60\%-12}$ irrigation treatment is the largest, with a maximum of 0.875, and followed by the $T_{80\%-21}$ and $T_{80\%-18}$ irrigation treatments, which are 0.856 and 0.818, respectively. The irrigation treatments with relative proximity greater than 0.8 were $T_{60\%-12}$, $T_{80\%-21}$ and $T_{80\%-18}$. Therefore, the best irrigation treatments are $T_{60\%-12}$, $T_{80\%-21}$ and $T_{80\%-18}$.

Table 3. TOPSIS evaluation calculation result.

Irrigation Scenarios	Positive Ideal Solution Distance D+	Negative Ideal Solution Distance D−	Relative Proximity C	Sort Result
$T_{100\%-12}$	1.778	0.257	0.126	16
$T_{100\%-15}$	0.875	0.978	0.528	8
$T_{100\%-18}$	0.770	1.097	0.588	7
$T_{100\%-21}$	0.665	1.209	0.645	6
$T_{80\%-12}$	0.533	1.303	0.710	5
$T_{80\%-15}$	0.437	1.419	0.765	4
$T_{80\%-18}$	0.343	1.538	0.818	3
$T_{80\%-21}$	0.278	1.652	0.856	2
$T_{60\%-12}$	0.252	1.768	0.875	1
$T_{60\%-15}$	1.656	0.245	0.129	15
$T_{60\%-18}$	1.540	0.319	0.172	14
$T_{60\%-21}$	1.424	0.411	0.224	13
$T_{40\%-12}$	1.323	0.566	0.299	12
$T_{40\%-15}$	1.210	0.665	0.355	11
$T_{40\%-18}$	1.096	0.768	0.412	10
$T_{40\%-21}$	0.985	0.876	0.471	9

3.5. Optimizing the Irrigation Scheduling

Through the simulation analysis of SWS, the total evapotranspiration and cumulative seepage, the average values of SWS under $T_{80\%-18}$ and $T_{80\%-21}$ irrigation treatments were

less than 1.00%, lower than that of $T_{100\%-12}$ treatment under fully irrigated conditions. The values of total evapotranspiration under the $T_{80\%-15}$, $T_{80\%-18}$ and $T_{80\%-21}$ irrigation schedules were close to the maximum of total evapotranspiration. The larger the evapotranspiration is, the better the turf grows. The cumulative seepage under $T_{80\%-18}$ irrigation treatment was lower than that under $T_{80\%-21}$ irrigation treatment. The analysis of the entropy-weighted-TOPSIS evaluation method showed that the optimal irrigation schedules were ranked in the top three results, namely, $T_{60\%-12}$, $T_{80\%-21}$ and $T_{80\%-18}$. In terms of comprehensive analysis, the irrigation amount of $T_{60\%-12}$ irrigation treatment is less than that of $T_{80\%-21}$ and $T_{80\%-18}$. Therefore, $T_{60\%-12}$ is the best irrigation treatment for turf irrigation schedule in the study region. Meanwhile, the optimization of the irrigation in this study is the result of the optimization of the model, and this result needs to be verified by field trials to change the irrigation schedule.

4. Conclusions

In this study, based on the water balance principle and RZWQM2, the characteristics of volumetric water content, field evapotranspiration and seepage change of turf were analyzed through a 2-year turf field experiment in 2020–2021, and the responses of soil water storage, evapotranspiration and seepage changes to different irrigation schemes were investigated. The mean values of volumetric water content of turf at the depth of 0–40 cm were 23.24% and 23.27% in 2020 and 2021, respectively. The turf evapotranspiration was greater during the turf peak growth period as a result of total evapotranspiration of 620.75 mm and 556.38 mm, accounting for 75.34% and 72.80% of the annual evapotranspiration in 2020 and 2021, respectively. The seepage values were 203.85 mm in 2020 and 278.89 mm in 2021. The validation results showed that RZWQM2 had good applicability for the simulation of turf water uses. The optimal turf irrigation schedule was explored by RZWQM2 and the optimal irrigation schedule was analyzed in conjunction with the entropy weight-TOPSIS evaluation method. The smallest difference in soil water storage (SWS) between the schedules and the fully irrigated treatment was observed when the irrigation water volume was 284.11 mm with 18 and 21 irrigation frequencies. Furthermore, the total evapotranspiration was very close to the full irrigation treatment under the 18 irrigation frequency. The best irrigation schedule obtained by the entropy weighted-TOPSIS evaluation method was $T_{60\%-12}$ (60% of the total irrigation amount and 12 irrigation frequency). Therefore, the best irrigation schedule was a 12 irrigation frequency with a total irrigation water volume of 213.08 mm.

This study comprehensively analyzed the changing characteristics of SWS, evapotranspiration and cumulative seepage under different turf irrigation amount and frequency, which can provide a scientific basis for guiding urban turf water-saving irrigation in semi-humid and semi-arid regions of China.

Author Contributions: Conceptualization, H.P. and H.Z.; methodology, H.Z.; software, H.Z.; validation, H.Z., H.P. and Y.S.; formal analysis, Y.S.; investigation, M.L.; resources, H.P.; data curation, H.Z.; writing—original draft preparation, H.Z.; writing—review and editing, H.Z.; visualization, J.W.; supervision, H.P.; project administration, H.Z.; funding acquisition, H.P. All authors have read and agreed to the published version of the manuscript.

Data Availability Statement: Not applicable.

Conflicts of Interest: The authors declare no conflict of interest.

References

1. Ding, Z.; Chen, Y.; Hu, C. Water Shortage and Water Shortage Types in China. *Spec. Zone Econ.* **2018**, *9*, 47–50.
2. NBSC (National Bureau of Statistics of China). *China Statistical Yearbook 2017*; National Bureau of Statistics Press: Beijing, China, 2017.

3. Pei, H.; Zhang, H.; Li, Y.; Liu, M.; Xiao, Y.; Wang, F. Characteristics and drivers of turf evapotranspiration in Northern China: A case study of turf (*Poa Pratensis*) in Zhangjiakou City, Hebei Province. *Water Sav. Irrig.* **2021**, *11*, 1–6.

4. Lu, C.; Deng, O.; Li, Y. A Study on Spatial Variation of Water Security Risks for the Zhangjiakou Region. *J. Resour. Ecol.* **2021**, *12*, 91–98.

5. Xuan, W.; Quan, C.; Shu, L. An optimal water allocation model based on water resources security assessment and its application in Zhangjiakou Region, northern China. *Resour. Conserv. Recycl.* **2012**, *69*, 57–65. [CrossRef]

6. Sevostianova, E.; Leinauer, B. Subsurface-applied tailored water: Combining nutrient benefits with efficient turfgrass irrigation. *Crop Sci.* **2014**, *54*, 1926–1938. [CrossRef]

7. Grabow, G.; Ghali, I.; Huffman, R.; Miller, G.; Bowman, D.; Vasanth, A. Water application efficiency and adequacy of ET-based and soil moisture–based irrigation controllers for turfgrass irrigation. *J. Irrig. Drain. Eng.* **2013**, *139*, 113–123. [CrossRef]

8. Fillo, N.K.; Bhaskar, A.S.; Jefferson, A.J. Lawn Irrigation Contributions to Semi-Arid Urban Baseflow Based on Water-Stable Isotopes. *Water Resour. Res.* **2021**, *57*, e2020WR028777. [CrossRef]

9. Jeong, H.; Pittelkow, C.M.; Bhattarai, R. Simulated responses of tile-drained agricultural systems to recent changes in ambient atmospheric gradients. *Agric. Syst.* **2019**, *168*, 48–55. [CrossRef]

10. Ma, L.; Ahuja, L.; Nolan, B.; Malone, R.; Trout, T.; Qi, Z. Root zone water quality model (RZWQM2): Model use, calibration, and validation. *Trans. ASABE* **2012**, *55*, 1425–1446. [CrossRef]

11. El-Sadek, A.N.; Salem, E.M.M. Simulation of wheat yield using the RZWQM as affected by supplemental irrigation in the North Western Coast of Egypt. *Eur. J. Agron.* **2016**, *38*, 279–292.

12. Zhang, H.; Ma, L.; Douglas-Mankin, K.R.; Han, M.; Trout, T.J. Modeling maize production under growth stage-based deficit irrigation management with RZWQM2. *Agric. Water Manag.* **2021**, *248*, 106767. [CrossRef]

13. Kuang, N.; Ma, Y.; Hong, S.; Jiao, F.; Liu, C.; Li, Q.; Han, H. Simulation of soil moisture dynamics, evapotranspiration, and water drainage of summer maize in response to different depths of subsoiling with RZWQM2. *Agric. Water Manag.* **2021**, *249*, 106794. [CrossRef]

14. Zhou, S.; Hu, X.; Ran, H.; Wang, W.; Hansen, N.; Cui, N. Optimization of irrigation and nitrogen fertilizer management for spring maize in northwestern China using RZWQM2. *Agric. Water Manag.* **2020**, *240*, 106276. [CrossRef]

15. Shrestha, S.; Manandhar, B. Evaluation of the Root Zone Water Quality Model (RZWQM) using field-measured data from the tropical zone, Thailand. *Water Air Soil Pollut.* **2014**, *225*, 1–14. [CrossRef]

16. Jeong, H.; Bhattarai, R. Exploring the effects of nitrogen fertilization management alternatives on nitrate loss and crop yields in tile-drained fields in Illinois. *J. Environ. Qual* **2018**, *213*, 341–352. [CrossRef]

17. Sun, M.; Huo, Z.; Zheng, Y.; Dai, X.; Feng, S.; Mao, X. Quantifying long-term responses of crop yield and nitrate leaching in an intensive farmland using agro-eco-environmental model. *Sci. Total Environ.* **2018**, *613*, 1003–1012. [CrossRef]

18. Li, Z.; Sun, Z. Optimized single irrigation can achieve high corn yield and water use efficiency in the Corn Belt of Northeast China. *Eur. J. Agron.* **2016**, *75*, 12–24. [CrossRef]

19. Zhang, K.; Shao, G.; Wang, Z.; Cui, J.; Lu, J.; Gao, Y. Modeling the impacts of groundwater depth and biochar addition on tomato production under climate change using RZWQM2. *Sci. Hortic.* **2022**, *302*, 111147. [CrossRef]

20. Hong, S.; Jiao, F.; Kuang, N.; Liu, C.; Ma, Y.; Li, Q. Simulating the effects of irrigation and tillage on soil water, evapotranspiration, and yield of winter wheat with RZWQM2. *Soil Tillage Res.* **2021**, *214*, 105170. [CrossRef]

21. Chen, X.; Qi, Z.; Gui, D.; Gu, Z.; Ma, L.; Zeng, F.; Li, L. Simulating impacts of climate change on cotton yield and water requirement using RZWQM2. *Agric. Water Manag.* **2019**, *222*, 231–241. [CrossRef]

22. Sadhukhan, D.; Qi, Z.; Zhang, T.; Tan, C.S.; Ma, L.; Andales, A.A. Development and evaluationof a phosphorus (P) module in RZWQM2 for phosphorus management in agricultural fields. *Environ. Model. Softw.* **2019**, *113*, 48–58. [CrossRef]

23. Allen, R.G.; Pereira, L.S.; Raes, D.; Smith, M. *Crop Evapotranspiration Guidelines for Computing Crop Water Requirements-FAO Irrigation and Drainage Paper 56*; FAO: Rome, Italy, 1998; Volume 300, p. D05109.

24. Qin, A.; Ning, D.; Liu, Z.; Li, S.; Zhao, B.; Duan, A. Determining threshold values for a crop water stress index-based center pivot irrigation with optimum grain yield. *Agriculture* **2021**, *1*, 958. [CrossRef]

25. Landa, F.M.; Fausey, N.R.; Nokes, S.E.; Hanson, J.D. Plant production model evaluation for the root zone water quality model (RZWQM 3.2) in Ohio. *Agron. J.* **1999**, *91*, 220–227. [CrossRef]

26. Ahuja, L.; Rojas, K.W.; Hanson, J.D. *Root Zone Water Quality Model: Modelling Management Effects on Water Quality and Crop Production*; Water Resources Publication: Littleton, CO, USA, 2000; pp. 13–50.

27. Ma, L.; Ahuja, L.R.; Bruulsema, T. *Quantifying and Understanding Plant Nitrogen Uptake for Systems Modeling*; CRC Press: Boca Raton, FL, USA, 2008.

28. Ma, L.; Hoogenboom, G.; Ahuja, L.R.; Ascough, J.C.; Saseendran, S.A. Evaluation of the RZWQM-CERES-Maize hybrid model for maize production. *Agric. Syst.* **2006**, *87*, 274–295. [CrossRef]

29. Teng, J.; Yasufuku, N.; Liu, Q.; Liu, S. Analytical solution for soil water redistribution during evaporation process. *Water Sci. Technol.* **2013**, *68*, 2545–2551. [CrossRef]

30. Fang, Q.; Yu, Q.; Wang, J. Simulating soil water dynamics and its effects on crop yield using RZWQM- CERES in the North China plain. *Acta Agron. Sin.* **2009**, *35*, 1122–1130. [CrossRef]

31. Gu, Z.; Qi, Z.; Ma, L.; Gui, D.; Xu, J.; Fang, Q.; Feng, G. Development of an irrigation scheduling software based on model predicted crop water stress. *Comput. Electron. Agric.* **2017**, *143*, 208–221. [CrossRef]

32. Legates, D.R.; McCabe, G.J. Evaluating the use of "goodness-of-fit" measures in hydrologic and hydroclimate model validation. *Water Resour Res.* **1999**, *35*, 233–241. [CrossRef]

33. Qi, Z.; Ma, L.; Helmers, M.J.; Ahuja, L.R.; Malone, R.W. Simulating nitrate-nitrogen concentration from a subsurface drainage system in response to nitrogen application rates using RZWQM2. *J. Environ. Qual.* **2012**, *41*, 289–295. [CrossRef]

34. Jiang, Y.; Zhang, L.; Zhang, B.; He, C.; Jin, X.; Bai, X. Modeling irrigation management for water conservation by DSSAT-maize model in arid northwestern China. *Agric. Water Manag.* **2016**, *177*, 37–45. [CrossRef]

35. Ding, J.; Hu, W.; Wu, J.; Yang, Y.; Feng, H. Simulating the effects of conventional versus conservation tillage on soil water, nitrogen dynamics, and yield of winter wheat with RZWQM2. *Agric. Water Manag.* **2020**, *230*, 105956. [CrossRef]

36. Malone, R.W.; Nolan, B.T.; Ma, L.; Kanwar, R.S.; Pederson, C.; Heilman, P. Effects of tillage and application rate on atrazine transport to subsurface drainage: Evaluation of RZWQM using a six-year field study. *Agric. Water Manag.* **2014**, *132*, 10–22. [CrossRef]

37. Liu, C.; Jiang, W.; Wu, Y.; Liu, Y.; Liang, L. Estimation of regional farmland irrigation water requirements and water balance in Northeast China. *Environ. Sci. Pollut. Res.* **2022**, *29*, 71840–71856. [CrossRef]

38. Liu, C.; Zhou, L.; Jia, J.; Wang, L.; Si, J.; Li, X.; Li, F. Maize yield and water balance is affected by nitrogen application in a film-mulching ridge–furrow system in a semiarid region of China. *Eur. J. Agron.* **2014**, *52*, 103–111. [CrossRef]

39. Zhou, H.; Zhao, W. Modeling soil water balance and irrigation strategies in a flood-irrigated wheat-maize rotation system. A case in dry climate China. *Agric. Water Manag.* **2019**, *221*, 286–302. [CrossRef]

40. Guo, C.; Zhang, Y.; Liu, Z.; Li, N. A Coupling Mechanism and the Measurement of Science and Technology Innovation and Rural Revitalization Systems. *Sustainability* **2022**, *14*, 10343. [CrossRef]

41. Kim, A.R. A study on competitiveness analysis of ports in Korea and China by entropy weight TOPSIS. *Asian J. Shipp. Logist.* **2016**, *32*, 187–194. [CrossRef]

42. Sun, Q.; Han, J.; Liu, S.; Zhou, L. The results of this study were similar to the results of soil moisture content changes in Sun Qiang's Beijing turf. *Acta Ecol. Sin.* **2005**, *25*, 1306–1311.

43. Braun, R.C.; Bremer, D.J.; Ebdon, J.S.; Fry, J.D.; Patton, A.J. Review of cool-season turfgrass water use and requirements: I. Evapotranspiration and responses to deficit irrigation. *Crop Sci.* **2022**, *62*, 1661–1684. [CrossRef]

44. Du, K.; Qiao, Y.; Zhang, Q.; Li, F.; Li, Q.; Liu, S.; Tian, C. Modeling soil water content and crop-growth metrics in a wheat field in the North China plain using RZWQM2. *Agronomy* **2021**, *11*, 1245. [CrossRef]

45. Fang, Q.; Ma, L.; Yu, Q.; Hu, C.; Li, X.; Malone, R.; Ahuja, L. Quantifying climate and management effects on regional crop yield and nitrogen leaching in the North China Plain. *J. Environ. Qual.* **2013**, *42*, 1466–1479. [CrossRef] [PubMed]

46. Ma, L.; Ahuja, L.R.; Saseendran, S.A.; Malone, R.W.; Green, T.R.; Nolan, B.T.; Bartling, P.N.S.; Flerchinger, G.N.; Boote, K.J.; Hoogenboom, G. A protocol for parameterization and calibration of RZWQM2 in field research. In *Methods of Introducing System Models into Agricultural Research*; American Society of Agronomy, Crop Science Society of America, and Soil Science Society of America: Washington, DC, USA, 2015; pp. 1–64.